A Study of Self-Excited Oscillations of the Tropical Ocean–Atmosphere System. Part I: Linear Analysis*

MARK A. CANE, MATTHIAS MÜNNICH AND STEPHEN E. ZEBIAK

Lamont-Doherty Geological Observatory of Columbia University, Palisades, New York

(Manuscript received 3 March 1989, in final form 27 December 1989)

ABSTRACT

We analyze the linearized version of an analytical model, which combines linear ocean dynamics with a simple version of the Bjerknes hypothesis for El Niño. The ocean is represented by linear shallow water equations on an equatorial beta-plane. It is driven by zonal wind stress,which is assumed to have a fixed spatial form. Stress amplitude is set to be proportional to the thermocline displacement at the eastern boundary.

It is shown that, for physically plausible parameter values, the model system can sustain growing oscillations. Both growth rate and period scale directly with the time that an oceanic Kelvin wave needs to cross the basin. They are quite sensitive to the coupling parameter between thermocline displacement and wind stress, and the zonal location and meridional width of the wind.

The most important parameter determining this behavior of the system is the coupling constant. For strong coupling the system exhibits exponential growth without oscillation. As the coupling is decreased the growth rate decreases until a transition value is reached. For smaller values of the coupling the growing modes of the system oscillate, with a period which is infinite at the transition value and decreases for decreasing coupling. The inviscid system has growing modes for any positive feedback, no mater how weak, though the growth rate rapidly becomes very small. For very weak coupling the period approaches the first resonance period of the free ocean. The model can also be expressed as a nondifferential delay equation. The components of this equation are easy to interpret physically and allow some insights into the nature of the oscillations. The relation of our results to other recent work and its implications for El Niño and the Southern Oscillation are discussed.

1. Introduction

Consider a rectangular tank containing a shallow layer of fluid. Fluid motions are driven by a stress parallel to one axis of the tank applied along a line parallel to the other axis. A float gauge at the tank wall toward which the stress is pointing is connected to the paddle wheel device supplying the stress, so that its amplitude and direction A depends on h_e, the fluid level there. What will be the nature of the resulting motions? In particular, will they be oscillatory?

The present paper addresses this question in the circumstance where the tank is in fact a basin situated on an equatorial beta plane with the zonally oriented walls infinitely far from the equator. (The nonrotating case is touched on briefly in section 4.) It is entirely concerned with the special case where the relation between the stress and the deviation of the fluid level from its mean height is linear; the richer behavior of the nonlinear case will be taken up in a sequel (Münnich et al. 1990). In the linear case the interesting question is the identity of growing modes, if any, with particular attention to whether or not they oscillate.

Arguably, the equatorial beta plane case is relevant to the El Niño–Southern Oscillation (ENSO) phenomenon, in accord with the view which regards ENSO as an oscillation of the coupled ocean–atmosphere system in the tropical Pacific (e.g., Bjerknes 1969; Cane and Zebiak 1985, 1987; Zebiak and Cane 1987; Schopf and Suarez 1988; Hirst 1988; Battisti 1988; Graham and White 1988). While one may question whether the problem examined here is an adequate paradigm for the ENSO cycle (and we will do so in the conclusion), there is considerable agreement that a model problem of this sort captures the essence of the numerical models recently put forward as models of ENSO.

We have in mind the numerical models of Zebiak and Cane (1987), Battisti (1988; this model is a close but not exact copy of that of Zebiak and Cane), and Schopf and Suarez (1988). The present paper adds to a second layer of work in which each numerical modeler tries to capture what he sees as the essential behavior of his rather complex grid point model of the ocean–atmosphere system in a model simple enough to be represented as a single equation in a single dependent variable with time as the only independent variable (cf. Battisti and Hirst 1988; Suarez and Schopf 1988; Schopf and Suarez 1989).

* Lamont-Doherty Geological Observatory Contribution Number 4622.

Corresponding author address: Dr. Mark Cane, Lamont–Doherty Geological Observatory, Columbia University, Palisades, NY 10964.

Not surprisingly, the complex model cannot be reduced to the simple one by a procedure which is entirely rigorous. As demonstrated in the papers of Schopf and Suarez (1989) and Battisti and Hirst (1989), however, a substantial part of the reduction can be accomplished before rigor must be abandoned in favor of heuristics. Rather than reprise the derivations in the works cited above, here we adopt a heuristic approach from the outset. The wellspring of all these models is the Bjerknes hypothesis (1966, 1972, and especially 1969; Cane 1986 is a recent summary). Briefly, if the eastern equatorial sea surface temperature (SST) warms, the thermal contrast between this region and the western Pacific will be reduced, thereby reducing the strength of the trades along the equator. The changes in ocean dynamics induced by the reduction in wind stress enhances the original warming: a positive feedback, resulting in the large anomaly often referred to as an El Niño or ENSO event. Bjerknes also pointed out that the normal phase, with a colder SST in the eastern Pacific and strong trades, is maintained by the same feedback loop operating in the opposite sense. The question Bjerknes left to us was what causes the transition from one state to the other. Thus we begin our analysis with a good idea of the source of instability but little idea of why it oscillates. While differing in detail, the works cited above all agree that adding the special properties of linear equatorial ocean dynamics to Bjerknes's scenario provide the answer.

The equation for temperature T in a well-mixed surface layer of depth h_s may be written (Zebiak and Cane 1987):

$$\frac{\partial T}{\partial t} + \bar{u}\cdot\nabla T + u\cdot\nabla(T+\bar{T}) + \frac{w}{h_s}[\bar{T}-\bar{T}_e+T-T_e(h)] + \frac{\bar{w}}{h_s}[T-T_e(h)] = Q_{sfc} = -\alpha_s T, \quad (1)$$

$$\frac{\partial T}{\partial t} + \mathrm{I} + \mathrm{II} + \mathrm{III} + \mathrm{IV} = -\alpha_s T$$

where overbars denote mean quantities and T_e is an entrainment temperature, here taken to depend only on the thermocline depth h. Equivalently, we are assuming that the vertical motion of all isotherms just beneath the mixed layer is entirely coherent with the thermocline motion. Four *dynamical* processes which can produce an SST warming may be enumerated: horizontal advection, either I, of warmer waters by mean surface currents, or II by anomalous currents; III, reduction of upwelling strength; and IV, a deepening of subsurface isotherms. Even with vertical velocities unchanged, the last mechanism warms SST because when the isotherms deepen the water entrained into the surface layer from below is warmer, than before. Bjerknes was unable to decide among the four. Detailed studies show that in the numerical models at least, while all are significant at some time or place during the ENSO cycle, it is the IV which is responsible for initiating the warming (Zebiak 1984; Battisti 1988). This lowering of the isotherms (equivalently, the lowering of the thermocline) is not a response to local wind changes: it is remotely forced. In view of the geometry of equatorial dynamics, packets of equatorial Kelvin waves, propagating eastward along the equator, must be the agent of change.

A body of work appears to contradict this result. Harrison and Schopf (1983) and Latif et al. (1988) have studied the warming due to a Kelvin wave initiated by a wind burst in the western Pacific and have all concluded that the heat flux associated with temperature advection by enhanced zonal currents will dominate over the upwelling effects. Given reasonable estimates for eastern Pacific horizontal and vertical temperature gradients, upwelling rates, and surface layer depths, the same conclusion follows inexorably from linear theory, which fixes the relative sizes of zonal velocity and isotherm displacement in a Kelvin wave.

The conclusion does not depend on the Kelvin waves being forced by a wind burst, but it does require that they be regarded as the outcome of some initial value (viz. Gill 1983) problem. If the Kelvin waves are a part of a low frequency periodic or quasi-periodic process then the result can be different. At low frequencies the resultant circulation is near equilibrium. In the eastern Pacific it consists of Kelvin waves plus the Rossby waves they generate when reflected at the eastern boundary (e.g., Cane and Sarachik 1981; henceforth CS). The zonal velocity signal, which must go to zero at the eastern wall, is near zero over a substantial zonal distance (how substantial is a function of frequency, cf. CS). By contrast, the isotherm displacements are enhanced over what they would be with Kelvin waves alone. Hence in the low frequency case, which involves eastern boundary reflections, the isotherm displacements are the dominant cause of temperature change—the result found in the analysis of the numerical model behavior. Even when the cycle is aperiodic, as in Zebiak and Cane (1987) and Schopf and Suarez (1988) each model event is an extreme phase of a cycle, connected to the last event and to the next event.

Diabatic heating is important in the surface thermal balance of the ocean. As first shown by Bjerknes (1969), however, it acts to damp the thermal anomalies created by ocean dynamics (also see Cane 1986). It is so effective at this that SST anomalies are in quasi-equilibrium in the eastern Pacific, determined by the balance between upwelling heat flux and heat exchange with the atmosphere, Q_s. Approximating Q_s as a linear damping of the temperature anomaly T this leaves

$$T = \frac{\bar{w}}{h_s\alpha_s + \bar{w}}\,T_e. \quad (1')$$

This balance is referred to as Model I by Hirst (1987, 1988; also see Battisti and Hirst 1989). The conse-

quence of interest here is that the SST variations on the equator are a function of isotherm displacement, with negligible time lags.

Drawing on results of Battisti's (1988) numerical model averaged over an eastern Pacific box (180°W to the South American coast, 2°N to 2°S); Battisti and Hirst (1989) attempt to account for all the terms in (1). They reduce (1) to the form

$$\left(\frac{1}{\alpha'}\frac{\partial}{\partial t}+1\right)T = b'T_e. \qquad (1'')$$

The consequences of the differences between (1′) and (1″) are considered in Appendix B (together with some other variations in model formulation). For now, we note that the difference between (1′) and (1″) does not lead to qualitative differences in overall model behavior. It does make notable quantitative differences, but, as will shortly appear, the same may be said of a number of model parameter variations.

The preceding discussion provides the basis for simplifying the ocean component of our model. The atmosphere responds to SST in the eastern equatorial Pacific. Although the effective SST patch extends off the equator, say from 10°S to 10°N, the source of the anomaly is water upwelled at the equator, which then spreads poleward by mean meridional advection and eddy diffusion. Ignoring the small time delay needed to accomplish this, the total SST anomaly is well represented by the SST at the equator. The discussion above motivates ignoring the influences of zonal advection and change of upwelling velocity, leaving equatorial SST as a function of isotherm displacements alone. (An alternative argument is that these displacements are an acceptable proxy for the other effects). The upper ocean movements have strong vertical coherence, so these displacements are related to anomalies in the thermocline depth, h. Hence $T_e = T_e(h)$. For the low frequency motions of interest to us thermocline depth anomalies are nearly constant within a few thousand kilometers of the eastern boundary (cf. CS). Hence they are all well approximated by h_e, the depth of the thermocline at the intersection of the eastern boundary and the equator. The SST anomaly (equivalently, all of the relevant ocean thermodynamics) is reduced to a function of the single ocean variable h_e. Linear shallow water dynamics will be used to determine h_e in response to the wind stress anomalies.

The wind stress anomaly is determined by the atmosphere model's response to the SST anomaly. In the models of Zebiak and Cane (1987) and Battisti (1988) the atmosphere is steady state, so the wind is in phase with the SST. For the more complex model of Schopf and Suarez, and the still more complex multilevel GCMs, the atmosphere is time dependent, but in fact the near equatorial winds respond very rapidly to tropical SST anomalies. Specifically, the response time is very short compared to the 2.3 months it takes an oceanic Kelvin wave to cross the Pacific. Here we take the wind stress anomaly to be simultaneous with the SST anomaly. We also take its spatial pattern $\tau(x, y)$ to be fixed in time. (The formalism we will use can easily accommodate a zonally propagating wind pattern, but beyond that it must be revised.) Though questionable as a representation of reality this is a decent approximation to the numerical model results and is additionally supported by the stability analysis of Hirst (1987). The particular pattern used here, however, is simpler than what the numerical models produce.

We now summarize the model discussion. The atmosphere model has been reduced to providing a relationship of the wind stress anomaly amplitude A to the SST anomaly. The SST anomaly depends only on the thermocline height at the eastern end of the equator. Hence all of the atmospheric dynamics and thermodynamics, and all of the ocean thermodynamics collectively boil down to a relation of the form $A(h_e)$. The ocean dynamics which relate h_e to the wind stress $A(t)\tau(x, y)$ are the linear shallow equations on an equatorial beta plane, simplified only by the standard low frequency approximation (cf. CS).

2. The model equations

Following the discussion in the Introduction, we arrive at a relation between wind stress A and eastern boundary thermocline displacement:

$$A = A(h_e) \qquad (2)$$

where the function A incorporates diabatic heating, meridional advection, upwelling velocities, the mean subsurface temperature structure $T(z)$, atmospheric heating, and tropical atmospheric dynamics. In the linear case to be studied here

$$A = \kappa h_e \qquad (3)$$

with κ a phenomenological coupling constant summarizing all processes by which the ocean affects the wind stress. It is the ratio of the change induced in the wind stress strength to the displacement of the thermocline in the eastern equatorial Pacific. Consistent with the Bjerknes scenario, the assumption is that wind changes A are ultimately related to dynamical ocean variations which can be "measured" by the thermocline displacement h_e.

The thermocline displacement is related to the wind through linear equatorial ocean dynamics. We take the ocean to be meridionally infinite, bounded by meridional walls at 0 and L_x. First we introduce nondimensional equivalents for the zonal and meridional distances x_d and y_d and time t_d:

$$x = \frac{x_d}{L_{eq}}; \quad y = \frac{y_d}{L_{eq}}; \quad t = \frac{t_d}{L_x/c}. \qquad (4)$$

Here L_{eq} is the usual equatorial radius of deformation, $L_{eq} = (c/\beta)^{1/2}$, where β has its usual meaning as the variation of the Coriolis parameter, and c is the wave

speed in this equivalent—one layer ocean. Note that the timescale is the time it takes for an equatorial Kelvin wave to cross the ocean, about 2.3 months for Pacific parameters (e.g., Cane and Moore 1981). Zonal distance is such that $0 \leqslant x \leqslant 1$. The wind stress is taken to be purely zonal with the form

$$Af(x)e^{-uy^2}e^{i\omega t}. \tag{5}$$

We resolve the ambiquity in the definiton of A by requiring

$$\int_0^1 f(x)dx = \frac{1}{x_E} \tag{6}$$

where

$$x_E = \frac{L_x}{L_{eq}}. \tag{7}$$

Thus, A is a measure of the wind strength which includes fetch effects (e.g., for wind stress patches with the same shape A is proportional to the patch width). The development given below could be extended to include propagating wind forms by taking $f(x)$ to be complex; the only modification required would be to the convention (6). If $\mu = 0.1$ then for Pacific parameters the meridional scale of the wind is about 15° of latitude, roughly the atmospheric radius of deformation (cf. Zebiak 1986). We will focus attention on $\mu = 0.2$ or $\mu = 0.1$—10° or 15°. CS were able to obtain a closed form solution for the response of an equatorial ocean to a wind stress of the form (5) in the case where $f(x)$ is constant; i.e., for all x

$$f(x) \equiv \frac{1}{x_E}. \tag{8}$$

Their solution requires that the long wave, low frequency approximation holds, which is met here. Equation (26) of CS (p. 662) gives the following expression for the Fourier transform of h_e:

$$h_e = \frac{A\left(\mu^{3/2} - \mu q(\mu, \omega) + i\int_0^\omega q(\mu, \omega')d\omega'\right)}{(1-\mu^2)\omega(i\sin(2\omega))^{1/2}} \tag{9}$$

where

$$q(\mu, \omega) = (\mu\cos 2\omega + i\sin 2\omega)^{1/2}. \tag{10}$$

Now $\mu^{3/2} = \mu q(\mu, 0)$ so the first two terms in (9) can be rewritten as

$$-\mu\int_0^\omega \frac{\partial q}{\partial \omega'}(\mu, \omega')d\omega' = \int_0^\omega \frac{\mu^2\sin(2\omega') - i\mu\cos(2\omega')}{q(\mu, \omega')}d\omega'.$$

Using this and (10), (9) becomes

$$h_e = \frac{A}{\omega}\left(\frac{i}{\sin(2\omega)}\right)^{1/2}\int_0^\omega \frac{\sin(2\omega')}{q(\mu, \omega')}d\omega'. \tag{11}$$

Now suppose the wind stress is again uniform but of limited fetch; i.e.,

$$f(x) = \begin{cases} \dfrac{1}{x_2 - x_1} & \text{if } x_1 \leqslant x \leqslant x_2, \\ 0 & \text{otherwise.} \end{cases} \tag{12}$$

The response may be found without further calculation by formally retracing the steps in the deviation of CS. The result analogous to (11) is

$$h_e = \frac{(i)^{1/2}A\int_{x_1\omega}^{x_2\omega}\frac{\sin(2\omega')}{q(\mu,\omega')}d\omega'}{\omega(\sin(2\omega))^{1/2}(x_2 - x_1)}. \tag{13}$$

By letting x_1, x_2 approach a common value x_0 we obtain the response to a delta function forcing at x_0, i.e., the Green function:

$$h_e = A\left(\frac{i}{\sin(2\omega)}\right)^{1/2}\frac{\sin(2\omega x_0)}{q(\mu, \omega x_0)} = AG(x_0; \mu, \omega). \tag{14}$$

Then for a general forcing $f(x)$

$$h_e = A\int_0^1 f(x')G(x'; \mu, \omega)dx' = A\left(\frac{i}{\sin(2\omega)}\right)^{1/2}\int_0^1 \frac{f(x')\sin(2x'\omega)}{q(\mu, \omega x')}dx'. \tag{15}$$

If we now insert the relation (2) (i.e, $A = \kappa h_e$) between the wind stress amplitude and the thermocline displacement into (15) we obtain a characteristic relation for the model, relating the period and growth rate given by the complex number ω to the coupling strength κ and the wind shape parameters:

$$1 = \kappa\int_0^1 G(x'; \mu, \omega)f(x')dx'. \tag{16}$$

3. Analysis of the characteristic relation

We are interested in the dependence on coupling strength and wind shape characteristics of the growth rate and period of the normal modes ($-\omega_i$ and $2\pi/\omega_r$, respectively, with $\omega = \omega_r + i\omega_i$). Figure 1 plots ($\omega_r$, ω_i) as a function of κ for a uniform wind patch covering the center half of the basin [i.e., Eq. (12) with $x_1 = 0.25$, $x_2 = 0.75$). For all $\kappa > 0$ there is a positive growth rate, although for $\kappa \leqslant 1$ it is very small. As κ approaches zero, the frequency approaches $\pi/2$, so the period becomes four times the Kelvin wave crossing time, which is just first resonance period for free waves (Cane and Moore 1981). As κ increases, the period increases, becoming infinite at $\kappa = \kappa_m \approx 1.5$. For $\kappa \geqslant \kappa_m$, the mode no longer oscillates and the growth rate increases rapidly with increasing κ. Not unexpectedly, period and growth rate are sensitive to the strength of the coupling between atmosphere and ocean.

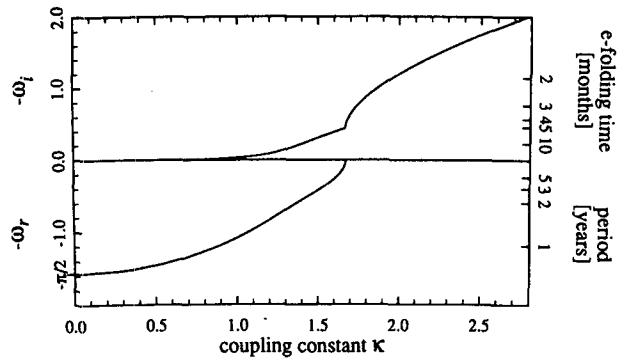

FIG. 1. Dependence of growth rate $-\omega_i$ and frequency ω_r on the coupling constant κ. Forcing parameters: $\mu = 0.1$, $x_1 = 0.25$, $x_2 = 0.75$.

Figure 2 is similar to Fig. 1, but shows a set of curves where the fetch $x_2 - x_1$ is varied. The clear impression is that ω is not very sensitive to fetch, as long as the zonal integral of the wind stress is unchanged [viz. (5)]. In Fig. 3, the meridional width is varied. The curves are qualitatively similar even as the scale varies from very narrow ($\mu = 0.99$, $L_y \approx 3°$) to very broad ($\mu = 0$, $L_y = \infty$). The most striking feature is the decrease in κ_m (the transition value from oscillatory to pure growth).

We now proceed to analyze these paremeter dependencies more systematically. The observation that the response is almost independent of fetch is valuable because it allows us to concentrate on a particular example of $f(x)$ with some confidence that our conclusions will apply more generally. A Green function is always useful because it allows a general solution like (15) to be written down. Depending on the problem, however, it may or may not represent the response to more realistic forms of $f(x)$. Figure 2 suggests that in our case it is, especially as we are most interested in relatively simple forms for the longitudinal dependence of the wind patch; e.g., a maximum amplitude at some central longitude, tapering off well before the boundaries. Relying on the mean value theorem, define x_c from the relation

$$G(x_c; \mu, \omega) = x_E \int_0^1 G(x; \mu, \omega) f(x) dx.$$

This is not terribly interesting if x_c varies considerably with ω, but if ω is small or the region where f is large is narrow then x_c will be nearly independent of ω and the response to $\delta(x - x_c)$ will closely approximate that to $f(x)$. Figure 2 illustrates how good our approximation can be; one would expect it to be even better for a more peaked form of $f(x)$. Henceforth we will restrict our analysis to the case $f(x) = \delta(x - x_c)$, in which case the relation (16) is

$$1 = \kappa G(x_c; \mu, \omega) \tag{17}$$

or

$$\kappa^2 = G^{-2} = \frac{\sinh(2\sigma)(\mu \cosh(2\sigma x_c) + \sinh(2\sigma x_c))}{\sinh^2(\sigma x_c)} \tag{18}$$

where $\sigma = i\omega$. In the special case where the wind is at $x_c = 1/2$, the center of the basin, $2\sigma x_c = \sigma$ and (18) simplifies to

$$\kappa^2 = \frac{2 \sinh\sigma \cosh\sigma(\mu \cosh\sigma + \sinh\sigma)}{\sinh^2\sigma}$$

or

$$\frac{\kappa^2}{2} = \cosh\sigma + \frac{\mu \cosh^2\sigma}{\sinh\sigma}$$

$$= \cosh\sigma + \mu \sinh\sigma + \frac{\mu}{\sinh\sigma}. \tag{19}$$

Let κ_m be the minimum value of κ for real σ (i.e., for pure growth) and σ_m be the corresponding growth rate. Hence

$$0 = \frac{\partial(\kappa^2)}{\partial\sigma}(\sigma_m) = \sinh\sigma_m + \mu \cosh\sigma_m - \frac{\mu \cosh\sigma_m}{\sinh^2\sigma_m}.$$

We claim that for $\kappa > \kappa_m$ the system shows only pure growth. Let $\sigma = \rho + i\omega$ with $\omega < \pi/2$. The imaginary part of $\kappa^2/2$ has to vanish. Calculating it from (19) gives

$$\mathrm{Im}(\kappa^2/2) = \sin\omega\left(\sinh\rho + \mu \cosh\rho - \frac{\mu \cosh\rho}{|\sinh\sigma|^2}\right).$$

For $\rho > \mathrm{Re}(\sigma_m) = \sigma_m$ we get by using (19) and (20) the following inequality

$$\frac{\mathrm{Im}(\kappa^2/2)}{\sin\omega} = \sinh\rho + \mu \cosh\rho - \frac{\mu \cosh\rho}{|\sinh\sigma|^2} > \sinh\rho$$

$$+ \mu \cosh\rho - \frac{\mu \cosh\rho}{\sinh^2\rho} > \sinh\sigma_m$$

$$+ \mu \cosh\sigma_m - \frac{\mu \cosh\sigma_m}{\sin^2\sigma_m} = 0$$

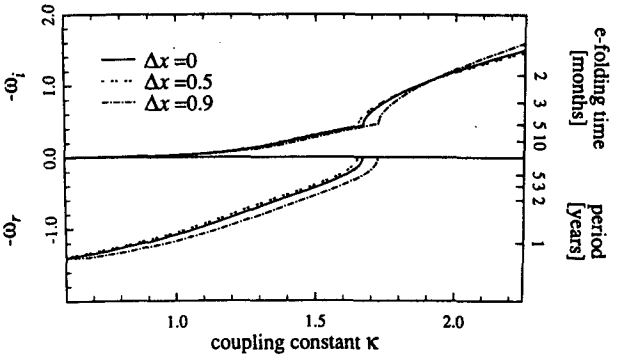

FIG. 2. Same as Fig. 1 but varying the longitudinal width $\Delta x = x_1 - x_2$ of the forcing, which is again centered in the middle of the basin.

or $\mathrm{Im}(\kappa^2/2) > 0$, if $\omega \neq 0$. So σ has to be real for $\mathrm{Re}(\sigma) > \sigma_m$. We want to find estimates for κ_m and σ_m for μ small. Rewrite (20) as

$$\mu = \frac{\sinh^3\sigma}{\cosh\sigma(1 - \sinh^2\sigma)}.$$

Since $\mu \ll 1$, we anticipate $\sigma_m \ll 1$ and expand in power series:

$$\mu = \frac{\sigma^3 + \frac{1}{2}\sigma^5 + \cdots}{\left(1 + \frac{1}{2}\sigma^2 + \cdots\right)(1 - \sigma^2 + \cdots)} = \sigma^3 + \sigma^5 + O(\sigma^7).$$

We invert to obtain the value σ_m at the transition:

$$\sigma_m \approx \mu^{1/3} - \frac{\mu}{3} + O(\mu^{5/3}). \tag{20}$$

And expanding (19) using (20) we find

$$\kappa_m^2 = 2 + 3\mu^{2/3} + O(\mu^{4/3}) \tag{21}$$

$$\kappa_m \approx (2 + 3\mu^{2/3})^{1/2} \tag{22}$$

which shows the weak dependence of κ_m on μ evident in Fig. 3: the narrower the scale ($\mu^{-1/2}$) the stronger the coupling must be to achieve pure growth. The growth rate varies like $\mu^{1/3}$: as the scale increases the growth rate approaches zero. The more equatorially confined the forcing the faster the growth in the oscillatory regime. For infinite scale the oscillations are neutral rather than growing.

We can see from Figs. 1–3 that the solutions of greatest interest—those which oscillate with long periods and relatively rapid growth rates—obtain for κ close to κ_m. We may analyze the behavior in the neighborhood of κ_m by approximating (19) for $\mu \ll 1$. In view of (20) σ will be small as well and so

$$\frac{1}{2}\kappa^2 \approx 1 + \frac{1}{2}\sigma^2 + \frac{\mu}{\sigma}. \tag{23}$$

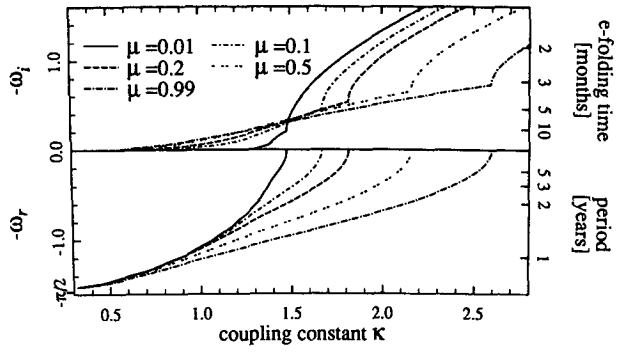

FIG. 3. Same as Fig. 1 but varying the meridional width parameter, μ.

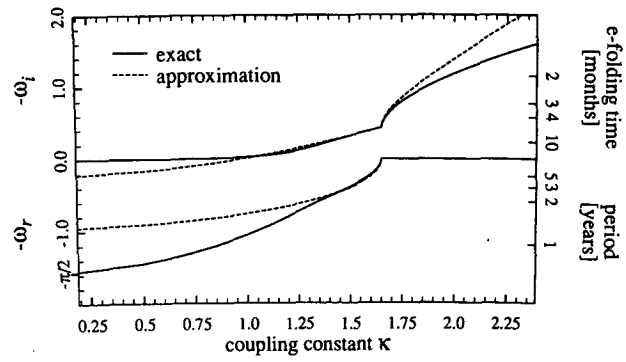

FIG. 4. Comparison of the exact function $\omega(\kappa)$ [Eq. (19)] with its approximation [Eq. (24)].

Expanding in a Taylor series about (σ_m, κ_m) yields

$$\kappa = \kappa_m + \frac{3}{2\kappa_m}(\Delta\sigma)^2 - \frac{\mu^{-1/3}}{\kappa_m}(\Delta\sigma)^3 + O((\Delta\sigma)^4) \tag{24}$$

where $\Delta\sigma = \sigma - \sigma_m$.

The cubic (24) may be solved for σ exactly, or approximately by writing $\Delta\sigma$ as a power series in $(\kappa - \kappa_m)^{1/2}$:

$$\sigma \approx \mu^{1/3}\left[1 - \frac{2}{9}\mu^{-2/3}\kappa_m(\kappa - \kappa_m)\right] \pm \left(\frac{2}{3}\kappa_m(\kappa - \kappa_m)\right)^{1/2}. \tag{25}$$

For $\kappa < \kappa_m$ the frequency goes to zero like the square root of $\kappa - \kappa_m$ and the growth rate is linear in κ. For a small range of κ the period varies over a very wide range. Figure 4 compares the approximation (24) with the exact Eq. (19): the fit is good in the vicinity of κ_m, and maintains good qualitative agreement until κ decreases to point where the approximations cross over and give decay instead of growth.

We complete the discussion of the centered case ($x_c = 0.5$) with an analysis of behavior for large and small κ. The former is straightforward: for $\kappa \gg 1$, $\sigma \gg 1$ so $\sinh\sigma \approx \cosh\sigma \approx e^\sigma$. Therefore (19) reduces to

$$\kappa^2 \approx 2(1 + \mu)e^\sigma \tag{26}$$

showing that the growth rate increases logarithmically with the coupling strength κ. To begin the analysis for $\kappa \ll 1$ again use $\sigma = i\omega$ and rewrite (19) as

$$\frac{\kappa^2}{2} = \frac{\cos^2\omega}{\sin\omega}[\tan(\omega) - i\mu]. \tag{27}$$

One may conclude immediately that for $\mu \neq 0$ and κ real there is no solution with ω real—no purely oscillating, neutral solution. If $\mu = 0$ then (26) reduces to $\cos\omega = \kappa^2/2$: pure growth for $\kappa > \kappa_m = (2)^{1/2}$ and

neutral oscillation for all $\kappa < (2)^{1/2}$. Hence for this case of infinite meridional scale there is no growing, oscillating mode.

In the more realistic case of finite meridional scale, $\mu \neq 0$, we have seen that for κ near κ_m there is a growing oscillating mode. By continuity, the growth rate must remain positive as $\kappa \to 0$. Since it is small, write $\omega = \omega_r - i\epsilon$, with ω_r, ϵ real and $\epsilon \ll 1$. Now expand $\sin\omega = \sin\omega_r - i\epsilon\cos\omega_r + O(\epsilon^2)$, etc. After some algebra, equating the real and imaginary parts of (27) yields the two equations

$$\cos\omega_r(1 - 2\mu\epsilon + \epsilon^2) = \frac{\kappa^2}{2} + O(\epsilon^3) + O(\mu\epsilon^2) \quad (28a)$$

$$\epsilon[1 - \cos^2\omega_r] = \mu\cos^2\omega_r + O(\mu\epsilon^2) + O(\epsilon^3). \quad (28b)$$

Since μ, $\epsilon \ll 1$, (28a) yields $\cos\omega_r = \kappa^2/2$. For $\kappa^2 \ll 1$

$$\omega_r \approx \frac{\pi}{2} - \frac{\kappa^2}{2} \quad (29a)$$

and

$$\epsilon \approx \frac{\mu}{4}\kappa^4. \quad (29b)$$

Thus as $\kappa \to 0$ the period approaches 4 rapidly—like κ^2—and the growth rate is very small. With some friction, i.e., Rayleigh friction of (small) magnitude r, there will be a neutral solution—an oscillation with constant amplitude—at $\epsilon = r$. From (28) the corresponding values of ω_r and κ are given by

$$\cos^2\omega_r \approx \frac{r}{r + \mu} \quad (30)$$

$$\kappa = \kappa_r \equiv \left(\frac{4r}{\mu}\right)^{1/4}. \quad (31)$$

In the frictional case with weak friction there are three regions:

1) $0 < \kappa < \kappa_r$: oscillation and decay.
2) $\kappa_r < \kappa < \kappa_m$: oscillation and growth.
3) $\kappa_m < \kappa$: growth without oscillation.

If the friction is strong enough (or the scale broad enough) so that $r > \mu^{1/3}$ then the oscillating modes ($\kappa < \kappa_m$) always decay. If $\kappa_m < \kappa < \kappa_r$ then the modes simply decay and $\kappa = \kappa_r$ allows a neutral stationary solution.

We have not yet considered the effect of moving the longitude of the wind patch from the center of the basin. Figure 5 demonstrates that this effect can be important, exerting a stronger influence than variations in zonal or meridional fetch. An analysis of the dispersion relation will augment the information in the figure. We return to the relation (18) and, anticipating that σ will be small, expand in powers of σ:

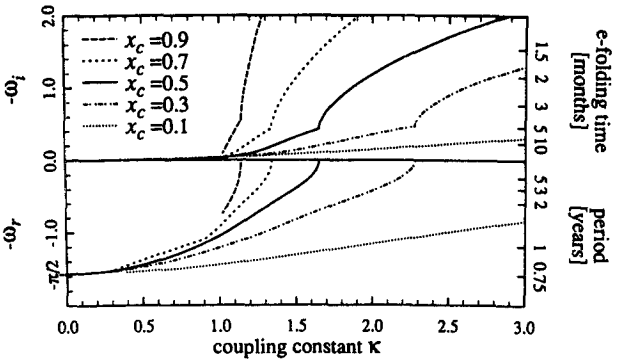

FIG. 5. Same as Fig. 1 but varying the center $x_c = (x_1 + x_2)/2$ of the forcing for constant width $\Delta x = 0.1$.

$$\kappa^2 = \frac{2\sigma + \frac{(2\sigma)^3}{3!} + \cdots}{2x_c\sigma + \frac{(2x_c\sigma)^3}{3!} + \cdots} + \mu\frac{\left(1 + \frac{(2x_c\sigma)^2}{2!} + \cdots\right)\left(2\sigma + \frac{(2\sigma)^3}{3!} + \cdots\right)}{\left(2x_c\sigma + \frac{(2x_c\sigma)^3}{3!} + \cdots\right)^2}$$

$$x_c\kappa^2 = 1 + \frac{2}{3}\sigma^2(1 - x_c^2) + O(\sigma^4) + \frac{\mu}{2x_c\sigma}\left[1 + \frac{2}{3}\sigma^2(1 + x_c^2) + O(\sigma^4)\right]. \quad (32)$$

As before, the value $\sigma = \sigma_m$ at the transition from pure growth to oscillation is at $\kappa = \kappa_m$, the minimum value of κ for σ real:

$$0 = \frac{2}{\partial\sigma}(x_c\kappa^2) = \sigma_m\cdot\frac{4}{3}(1 - x_c^2) - \frac{\mu}{2x_c\sigma_m^2} + O(\mu) + O(\sigma^3)$$

$$\sigma_m(x_c) \approx 2\left(\mu\frac{(x_c - x_c^3)}{3}\right)^{1/3} \quad (33)$$

$$\kappa_m^2(x_c) \approx \frac{1}{x_c}\left[1 + \frac{3}{2}\mu^{2/3}\left(\frac{1 - x_c^2}{3x_c^2}\right)^{1/3}\right]. \quad (34)$$

This dependence on x_c is illustrated in Fig. 6. For $x_c = \frac{1}{2}$ the previous results for the centered case (21), (22) are recovered. The values of σ_m and κ_m do not change markedly from the centered results until the boundaries are closely approached. At both boundaries the growth rate becomes infinite, but at the western boundary ($x_c = 0$) the transition coupling strength κ_m also becomes infinite so pure growth is never attained. In contrast, at the eastern boundary ($x_c = 1$) $\kappa_m = 1$ for all μ, so the pure growth regime begins at a relatively

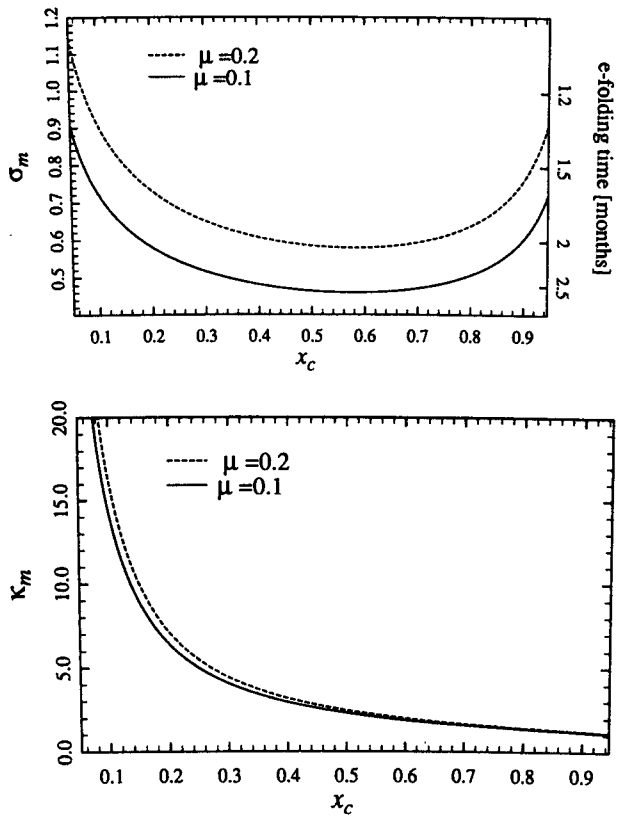

FIG. 6. (a) Plot of Eq. (31): minimal growth rate for pure growth, σ_m, as a function of the longitude of the forcing, x_c. (b) Plot of Eq. (32): minimal coupling constant for pure growth, κ_m, as a function of the longitude for the forcing, x_c.

low coupling strength. While the transitional coupling strength decreases monotonically from west to east across the basin, the transitional growth rate is a minimum just east of the central longitude at $x_c \approx \sqrt{3}/3$.

The behavior in the vicinity of κ_m may be found as for the centered case [(24)ff]. With $\Delta\sigma = \sigma_m$ using (33), (34) we obtain

$$2\kappa_m(\kappa - \kappa_m) = 2\frac{1 - x_c^2}{x_c}(\Delta\sigma)^2 - \frac{\mu^{-1/3}}{2x_c^2}\left(\frac{3}{8x_c(1 - x_c^2)}\right)^{4/3}(\Delta\sigma)^3. \quad (35)$$

As long as x_c is not close to the boundaries the qualitative behavior is similar to the centered case [e.g., (25)]: as $\kappa \to \kappa_m$ from below the frequency approaches zero like $(\kappa_m - \kappa)^{1/2}$ and the growth rate increases linearly with κ. Again, the period ranges over a wide range for small variations in coupling strength.

For small κ the off-center forcing allows for some different behavior than the centered case. For example, it becomes possible to have neutral, oscillating solutions even in the absence of friction. To see this write (18) in a form similar to (27):

$$\kappa^2 = [-i\mu\cos(2x_c\omega) + \sin(2x_c\omega)]\frac{\sin(2\omega)}{\sin^2 x_c\omega}. \quad (36)$$

For a neutral solution ω is pure real. If κ is also real and nonzero, then $\cos 2x_c\omega = 0$. The longest period neutral solution is

$$\omega = \frac{\pi}{4x_c}. \quad (37)$$

It occurs at $\kappa = \kappa_n$; from (36),

$$\kappa_n^2 \equiv 2\sin\left(\frac{\pi}{2x_c}\right). \quad (38)$$

We require $\kappa^2 > 0$, which is possible only if $x_c > 1/2$—if the forcing is in the eastern half of the basin. For $x_c \leq 1/2$ the oscillating solutions are all growing. A more general result for $\kappa \ll 1$ can be obtained by letting $\omega = \pi/2 - \omega'$ with $\omega' \ll 1$ in (36):

$$\frac{\kappa^2}{2}\sin^2(\pi x_c) = [i\mu\cos(\pi x_c) + \sin(\pi x_c)]\omega' + O(\omega'^2). \quad (39)$$

The results comparable to the centered case [cf. (28)] are

$$\mathrm{Re}(\omega) = \frac{\pi}{2} - \frac{\kappa^2}{2}\left(\frac{\sin^3\pi x_c}{\mu^2 + (1 - \mu^2)\sin^2\pi x_c}\right) \quad (40)$$

so the resonant frequency, $\pi/2$, is approached ever more rapidly as the forcing is moved further off center; and

$$-\mathrm{Im}(\omega) = \frac{\mu\kappa^2}{2}\left(\frac{\sin^2(\pi x_c)\cos(\pi x_c)}{\mu^2 + (1 - \mu^2)\sin^2(\pi x_c)}\right) \quad (41)$$

implies decay for $x_c > 1/2$. At $x_c = 1/2$ $\mathrm{Im}(\omega)$ vanishes according to (41); to recover (28b) one must go to the next order in ω'. Note that it also vanishes at the end points $x_c = 0$ and $x_c = 1$ [although not rapidly since the denominator becomes $O(\mu^2)$]. In general, the $x_c = 0$ and $x_c = 1$ cases exhibit a number of idiosyncratic behaviors which require special analysis. Since this situation with the delta function forcing precisely on the boundary is so strange and not of interest to us we shall not pursue it.

At $x_c = 1/2$, the neutral mode period occurs in the limit $\kappa = 0$; it is just the period of the free resonant mode (cf. Cane and Moore 1981). As the forcing is moved east the neutral mode period grows longer, becoming twice as long for $x_c = 1$ (the eastern boundary). For $x_c > 1/2$, the neutral mode occurs at a positive coupling strength κ_n. For $\kappa < \kappa_n$ the modes are oscillating and decaying. As $x_c \to 1$, κ_n approaches 1 from below while according to (32) κ_m approaches 1 from above. Hence as the forcing is moved farther to the east, the

range of coupling strengths that allow both oscillation and growth narrows: the likely possibilities become oscillation and decay ($\kappa < \kappa_n$) or pure growth ($\kappa > \kappa_m$); viz., Fig. 5 for $x_c = 0.9$.

4. Relation to delay equations

Recently, Battisti and Hirst (1988), Suarez and Schopf (1988), and Schopf and Suarez (1989) have developed "analogue" models of more complete ENSO models. The implication in these papers is that a delayed response is the essence of the oscillation. The mechanism is roughly as follows. An eastward wind patch forces a downwelling Kelvin wave which propagates east, lowers the thermocline, raises SST, thus enhancing the eastward wind. This direct link is very much the Bjerknes (1969) mechanism as filled out by Wyrtki (1975). It alone seems to imply nonoscillating growth, but the same wind excites Rossby waves which raise the thermocline [cf. Battisti (1988) or Schopf and Suarez (1989) or Cane and Zebiak (1987)]. Since mass is conserved, some such "cold" signal inevitably accompanies the warm Kelvin wave. Since they are Rossby waves, they travel westward to the boundary, and then are reflected as a Kelvin wave. When this arrives at the east, it "shuts down" the positive feedback of the direct link, resulting in an oscillation. We wish to explore the role of delays, but first we show that our model involves the same direct and delayed responses.

On one level this is obvious, since the heart of all these models is the same linear shallow water equatorial beta plane dynamics. To see how it is embodied in our equations, return to (14) rewritten in terms of

$$z = e^{-i\omega} \tag{42}$$

as

$$h_e = \frac{z^{-2x_c} + z^{2x_c}}{\{(z^{-2} - z^2)[(1+\mu)z^{-2x_c} - (1-\mu)z^{2x_c}]\}^{1/2}} A. \tag{43}$$

Define

$$\nu = \frac{1-\mu}{1+\mu} \tag{44}$$

multiply through by $z[z^{-2} - z^2]^{1/2} = [1 - z^4]^{1/2}$ and rearrange to obtain

$$h_e = [1 - (1 - z^4)^{1/2}]h_e + \frac{z^{1-x_c}(1 - z^{4x_c})}{[(1+\mu)(1 - \nu z^{4x_c})]^{1/2}} A. \tag{45}$$

Expanding this in power series gives

$$h_e = \sum_{n=1}^{\infty} a_n^+ z^{4n} h_e + \frac{z^{1-x_c} + z \sum_{n=1}^{\infty} z^{(4n-1)x_c}(a_n^- \nu^n - a_{n-1}^- \nu^{n-1})}{(1+\mu)^{1/2}} A \tag{46}$$

where $a_n^{\pm}$ are the absolute values of the coefficients of x^n in the expansions of $(1-x)^{\pm 1/2}$.

Now we interpret ω as the Fourier transform variable resulting from a transform in time. Then in (45) h_e and A are to be interpreted as variables in the frequency domain. Obtaining an equation in the time domain from (45) requires inverting only operators of the form z^a. Since $z^a \hat{f}(\omega)$ transforms to $f(t-a)$ it is easy to see that the result is

$$h_e(t) = \frac{1}{(1+\mu)^{1/2}} A[t - (1 - x_c)] + \frac{\sum_{n=1}^{\infty} [a_n^- \nu^n - a_{n-1}^- \nu^{n-1}]}{(1+\mu)^{1/2}} A[t - (4n-1)x_c - 1] + \sum_{n=1}^{\infty} a_n^+ h_e(t - 4n).$$

The first term is the Kelvin wave forced at $x = x_c$ which travels directly to the eastern boundary at $x = 1$. The second is the sum of the odd Rossby waves; wave $2n - 1$ takes a time $[2(2n-1) + 1]x_c$ to travel from the forcing longitude x_c to the western boundary at $x = 0$. There it is reflected eastward as a Kelvin wave, which takes an additional 1 time unit to cross to the east. The last term on the righthand side of (46) adds the effect of all the Rossby waves previously generated at the eastern boundary as the reflection of incident Kelvin waves. We note that the development of (46) from (14) is a reversal of the procedure in CS: here we have recovered the infinite series arising naturally in the forced problem from the closed form Green function (also, cf. Schopf and Suarez 1989).

We are tempted to think of the oscillation as a consequence of the delays in (46), but further investigation indicates that the matter is not straightforward. In fact there are related systems with delays which do not allow oscillating, growing modes. Consider a nonrotating system setup as in the previous case; i.e., driven by a stress of the form $\kappa h(t)\delta(x - x_c)$, where h is the height at the east (right) end of the basin $x = 1$. Assume a uniform mean eastward current U and let $\alpha = (1+U)/(1-U)$. Then α is the ratio of the speed of the eastward traveling wave, here called a K-wave, to the speed of the speed of the westward traveling R-wave. Also we will allow for imperfect relations at the boundaries: The reflection coefficients r_w at the west and r_e at the east may be less than 1. As shown in appendix A:

$$h(t) = \kappa h[t - (1 - x_c)] - r_w \kappa h[t - (1 + \alpha x_c)] + r_e r_w h[t - (1 + \alpha)]. \tag{47}$$

The terms on the right-hand side are easily interpreted: The first one is the contribution of the forced K-wave at x_c that hits the boundary after a time of $1 - x_c$. The next term represents the forced R-wave that needs the time αx_c to reach the western boundary where

it gets converted to a K-wave and gets to the east after 1 additional time unit. It has the opposite sign and acts as a restoring force. The last term comes from the wave that got reflected at the east and crossed the basin back and forth as an R-wave and then a K-wave. Judicious choices for α, r_w and r_e will make (47) equivalent to the equatorial beta plane Eq. (46) with just a single ($n = 1$) Rossby wave [also see appendix B].

Most studies of the nonrotating system take $r_e = r_w = 1$ and $U = 0$ so $\alpha = 1$. In the case it can be shown (appendix A) that the delay equation (47) has no oscillating, growing solutions. As on the beta-plane with infinite width forcing ($\mu = 0$) solutions are either neutral and oscillating or pure growth.

The implication is that something more particular to the beta plane system (47) than the delays per se must be important for the oscillation. Cane and Zebiak (1987) argued that the asymmetry of the reflection process at the east and west was critical. At the west, Rossby waves at all latitudes reflect as an equatorially confined Kelvin wave, so the negative Rossby wave signal is efficiently guided to the eastern side. At the east, the Kelvin wave signal does not accumulate at the critical area near the equator; instead, the reflection process spreads it to high latitudes. In fact, the reflection process is so effective at removing mass that Schopf and Suarez (1988) and Battisti and Hirst (1989) ignore it without much ado, treating the boundary as if the Kelvin wave just went through it; i.e., as if $r_e = 0$.

If we model this asymmetry by setting $r_e = 0$, while keeping the wave speeds the same ($\alpha = 1$) growing oscillating solutions to (47) are possible (see appendix A). This would seem to support the idea presented above, which might be phrased as saying that the eastern boundary reflection is important for what it does not do. (cf. Cane and Zebiak 1987).

We have not yet, however, isolated the other special feature of the equatorial wave system, the difference in speed between eastward and westward propagating waves. We restore the perfect reflections to (47), $r_e = r_w = 1$, and now take $\alpha = 3$, the ratio of the speed of a Kelvin wave to an $n = 1$ Rossby wave. Again, the resulting system contains oscillating, growing modes.

We want to give a heuristic explanation for the occurrence of growing oscillations. Rescale time by $1 - x_c$, the time a K-wave needs to reach the eastern boundary, and define $T = (1 + \alpha)/(1 - x_c)$ which is the free period in the new units. Then (47) becomes

$$h(t) = \kappa h(t-1) - \kappa r_w h[t - (T - \alpha)] + r_w r_e h(t - T). \quad (48)$$

We restrict ourself to integer α's and analyze (48) term by term. Consider first the case of $r_w = 0$. Then only the first term remains and (48) reduces to a single feedback equation $h(t) = \kappa h(t-1)$. This equation allows only pure growth (decay) for $\kappa > 1 (< 1)$. Next we take $r_e = 0$, or that the last term of (48) vanishes:

$$h(t) = \kappa h(t-1) - \kappa r_w h(t - \tau) \quad (49)$$

with $\tau = T - \alpha$. For an initial disturbance ($h(t) = 0$ for $t < 0$; $h(0) = 1$) we get the following time sequence for h (assuming that τ is an integer N).

$$1, \kappa, \kappa^2, \ldots, \kappa^{N-1}, \kappa^N - r_w\kappa, \kappa^{N+1} - 2r_w\kappa^2, \kappa^{N+2} - 3r_w\kappa^3, \kappa^{N+3} - 4r_w\kappa^4, \ldots, \kappa^{2N-1} - 2Nr_w\kappa, \kappa^{2N} - (2N+1)r_w\kappa + r_w^2, \ldots. \quad (50)$$

Note how the restoring effect of the forced R-wave accumulates: At $t = N$ the R-wave from $t = 0$ diminishes the exponential growth of h by r_w. At the next time step this reduction gets amplified to κr_e and adds up with reduction of the same amount by the R-wave excited at $t = 1$. The reductions accumulate so they can make the sequence decreasing. As long as r_w is not too small and κ not too large this accumulating reduction can lead to an oscillation despite the fact that each individual R-wave component is smaller than the K-wave component forced at the same time. As an example we set $r_w = 1$; $\kappa = 1$, $\alpha = 3$ (so that $T = 6$, $N = 5$). The resulting time sequence is

$$1, 1, 1, 1, 1, 0, -1, -2, -3, -4, -5, -5, -4, -2, 1, \ldots. \quad (51)$$

Now we consider the case of $r_e > 0$ and for simplicity set $r_w = 1$. In appendix A we show growing oscillations if either $r_e < 1$ or $\alpha > 1$. In the beginning the sequence (49) remains the same (with $r_w = 1$):

$$1, \kappa, \kappa^2, \ldots, \kappa^{N-1}, \kappa^N - r_w\kappa, \kappa^{N+1} - 2r_w\kappa^2. \quad (52)$$

At $t = T$ the waves that were reflected from the eastern boundary alter the series:

$$h(T) = \kappa^T - (T - N + 1)\kappa^{T-N+1} + r_e$$

$$h(T+1) = \kappa^{T+1} - (T - N + 2)\kappa^{T-N+2}\kappa^{T-N+2} + 2\kappa r_e$$

$$h(T+2) = \kappa^{T+2} - (T - N + 3)\kappa^{T-N+3}\kappa^{T-N+3} + 3\kappa r_e. \quad (53)$$

As we see the effect of the reflected wave accumulate in the same fashion as the forced R-wave, reducing the restoring effect of the R-wave. If the speeds for R- and K-wave are the same we have $\alpha = 1$, $T - N = 1$, so that this happens right away. There is no time for the R-wave to accumulate without reduction by the eastern boundary reflections and for perfect reflection the accumulation of the forced R-wave is cancelled completely—no growing oscillation can occur. So we obtain, for example, for $r_e = 1$, $\alpha = 1$, $x_c = \frac{1}{2}$ ($N = 5$, $T = 6$), the time sequence

$$1, 1, 1, 1, 1, 0, 0, 0, 0, 0, 1, 1, 1, 1, 1, 0, \ldots$$

which shows no growing oscillation. If $r_e < 1$ the cancellation is only partial. The restoring effect of the R-

wave is weakened, but growing oscillations are still possible. For $r_e = \frac{1}{2}$ and other parameters as in the previous example, we get

$$1, 1, 1, 1, 1, 0, -.5, -1, -1.5, -2, -1.5,$$
$$-1, -0.25, -0.75, 2, 2.5, \ldots.$$

Another way to get a growing oscillation is if the R-wave is slower than the K-wave ($\alpha > 1$). Then the reduction by the eastern reflection is delayed, giving the R-waves some time to accumulate. For $\alpha = 3$, $r_e = 1$ we obtain the sequence ($x_c = \frac{1}{3}$)

$$1, 1, 1, 1, 1, 0, -1, -2, -2,$$
$$-2, -1, -1, 4, 6, 7, 6, \ldots.$$

5. Summary and discussion

In this paper we have investigated the behavior of a simple coupled tropical ocean–atmosphere model. The ocean component is described by the inviscid shallow water equations on a meridionally infinite equatorial beta plane. It is driven by a wind stress of the form $A(t)f(x)\exp(-\mu y^2)$, with the amplitude A linearly related to the equatorial height anomaly at the eastern end of the basin: $A(t) = \kappa h(x = 1, y = 0, t)$.

The governing equations are solved analytically and the influence of various parameters is examined. We are particularly interested in the circumstances which allow the existence of unstable, oscillating modes of this self-excited system. If the coupling between the ocean and atmosphere is very strong then the most unstable modes do not oscillate. In most cases, once the coupling κ falls below a threshold value κ_m, which depends on other parameters, then there are growing modes which oscillate at low frequency (Fig. 1). The period is infinite at $\kappa = \kappa_m$, decreasing as κ decreases. In some cases the unstable modes exist for all $\kappa > 0$, with the period approaching that for the resonant mode of the shallow water ocean (four times the time for an equatorial Kelvin wave to cross the ocean basin) as $\kappa \to 0$. Hence the period ranges between 4 (about 9 months for Pacific parameters) and infinity. There is no low frequency cutoff: in the absence of friction there is some growth even for vanishingly weak coupling, though it does become small as κ departs from the transition value κ_m. For κ near κ_m, the period of the growing oscillations is very sensitive to the value of the coupling strength.

Behavior is somewhat dependent on the mean longitude x_c of the wind stress, but is otherwise nearly independent of its zonal variations; the wind fetch, for example (Fig. 2). This result occurs because the time it takes for a Kelvin wave to cross the wind patch is short compared with the period and e-folding time of the unstable modes of interest. It allows us to simplify the analysis by considering only the form $f(x) = \delta(x - x_c)$; i.e., the forcing is concentrated at the mean longitude.

If the wind is centered in the western half of the basin then the situation is as described in the previous paragraph: growth is possible for all $\kappa > 0$. If the wind is centered in the eastern half of the ocean then growing oscillating modes no longer exist at small κ; even in the absence of friction there can be a neutral mode. The further east the forcing is centered, the narrower the range of κ that admits growing oscillating solutions. In the extreme case where it is concentrated on the eastern boundary the only oscillating modes are neutral. The value of κ_m increases as the central longitude x_c is moved westward, permitting oscillating modes for a broader range of coupling strengths. In the limit where the forcing is on the western boundary unstable oscillating modes exist for all κ (Fig. 6b). All other things, such as the coupling strength, being equal, the growth rate and period increase as the wind center moves east (Fig. 5).

Behavior also changes with the meridional scale of the forcing (Fig. 3): for fixed κ as the meridional scale increases the period of the oscillating modes increases while their growth rate is almost unchanged. Also, as the scale increases κ_m, the maximum coupling value allowing oscillation, becomes smaller. At the extreme where the forcing is independent of latitude the oscillating modes are no longer unstable.

Our model joins those of Battisti and Hirst (1989) and Suarez and Schopf (1988) in a class of one-equation models offered as a paradigm for ENSO. All are based on experience with numerical models which were able to simulate aspects of the ENSO cycle, though none of the reduced models can be said to be rigorously derived from their more elaborate predecessors. As noted in the Introduction, all combine linear equatorial shallow water ocean dynamics with a stripped down version of Bjerknes' ideas on the two-way coupling of the ocean and atmosphere in the equatorial Pacific. Bjerknes' original scenario for the genesis of ENSO events was confined to an equatorial x–z plane; adding equatorial ocean dynamics makes a crucial connection to higher tropical latitudes.

All of the models exhibit unstable oscillations at the several year periods characteristic of the observed ENSO cycle. The collective behavior of these somewhat different models adds weight to the thesis that the Bjerknes feedback plus linear equatorial ocean dynamics captures the essence of the ENSO cycle. At present, there is no equally complete or convincing paradigm for other suggestions as to the nature of ENSO (e.g., random events, in some accounts triggered by westerly bursts; the oscillation is created by the seasonal cycle; extratropical origins.)

The models differ in detail and their authors occasionally differ in interpretation of the results. For example, Schopf and Suarez (1988) argue that there should be a high frequency cutoff for the unstable modes at a period which is twice the resonance period (i.e., eight times the Kelvin crossing time). Our results

show no such cutoff, though some cases exhibit a rapid dimunition of growth rate at about this period. Our results suggest to us that such a cutoff is not implicit in the fundamental ENSO mechanism. Battisti and Hirst (1989) argue that ENSO is essentially a linear oscillation on the grounds that their best estimate of reduced model parameters yields the period of about 4 years characteristic of their version of the Zebiak and Cane (1987) model. We have found that the period of the unstable modes found here is highly sensitive to a number of model parameters, including the strength of the coupling from ocean to atmosphere, the longitudinal position of the wind, and its meridional scale. Such results are quite similar to those in BH, which also indicate that the period is very sensitive to parameter variations. This sensitivity is especially marked in the neighborhood of the 4 year period (e.g., Fig. 1). Additionally, our best estimate of parameters in the Zebiak and Cane model [$\kappa \approx 2$; $\mu \approx 0.2$] puts our reduced model in the regime of pure growth. Since none of the parameters can be precisely determined from the numerical models—none are truly constant within the model—we do not agree that the linear paradigm is sufficient to determine the period. Results to be reported in Münnich et al. (1990) indicate that plausible nonlinear relations between height and wind stress tend to narrow the range of periods which occur.

The reduced models of Battisti and Hirst (1989) and Suarez and Schopf (1988) are both differential delay equations. Ours may be cast in this form as well, though in the case most studied here where the wind has a vanishingly narrow zonal scale, a pure delay equation results. This is the response to a delta function forcing, a Green's function. The response to a finite width forcing $f(x)$ would bring in integrals, and differentiating the result would produce a differential delay equation. (The absence of differential terms in our model is a consequence of the neglect of the travel time across the forcing region.)

The concept of delays is helpful in understanding the oscillations, but there are subtleties. The obvious nonrotating version of our model, whose mathematical form is also a delay equation, does not have unstable oscillating modes. (It resembles the equatorial case where the wind is independent of y.) Such modes exist, however, if the reflection coefficient at the east is made less than 1 or if westward propagating waves are slower than eastward ones. For the nonrotating case the answer to the question posed in the opening paragraph of this paper is that in order to have oscillating growing modes either the eastern end of the tank must be leaky or a mean eastward current must be flowing through it.

The explanation we can provide for the model behavior has similarities with a number of previous ones, particularly Cane and Zebiak (1985), Battisti and Hirst (1988), Schopf and Suarez (1988) and Cane and Zebiak (1987), most closely resembling the last of these. We begin at a point where the wind stress perturbation, which is related to the ocean height at the eastern end of the equator, is eastward. The ocean responds with a height rise to the east of the forcing and a fall to the west. The pairing of the rise and fall is inescapable, a consequence of mass conservation. The rise propagates eastward along the equator in the form of an equatorial Kelvin wave. The fall moves westward more slowly and more broadly, as a packet of Rossby waves.

The rapidly moving rise soon comes to the eastern boundary, enhancing the eastward stress by adding to the height there. By itself, this positive feedback, which is at the core of Bjerknes's scenario, would give only the pure growth Bjerknes envisioned. There would be no oscillation, but there is also the signal associated with the fall. It propagates westward as Rossby waves until the western boundary is encountered, at which point it is reflected back along the equator as a Kelvin wave. When this negative height signal reaches the eastern end of the ocean it competes with the directly forced positive Kelvin wave signal. If it wins then the amplification of the eastward wind stress will be arrested, and the height at the east can diminish further and eventually become negative; an oscillation is possible.

When will the indirect, delayed signal win? If the coupling is too strong then the direct Kelvin signal, having benefited from the added growth during the delay period, will be too strong to be headed, and unbridled growth ensues. This is just our result for $\kappa > \kappa_m$. (Recall that as the forcing moved east, increasing the delay period, secular growth was achieved at weaker coupling and unstable oscillations became less likely. The same result obtained as the meridional scale of the forcing increased; by enhancing the importance of higher Rossby waves the mean speed is decreased so the effective delay is increased.) It is as if only the Kelvin wave were forced in the first place; the Rossby waves are able merely to dilute the growth.

An interesting contrast can be imagined by hypothesizing that only Rossby waves are directly forced. Now the forced signal, comprised of Rossby waves, would always be opposite in sign to the height at the east determining the forcing. Growth is possible, but the out of phase relationship between forcing and ocean response means it cannot be of one sign. Oscillations are unavoidable. One might consider the forced Kelvin wave as an impediment for the oscillations. As its relative contribution increases, the period increases, leading finally to pure growth. One might now wonder how the Rossby waves can succeed. Their combined amplitude is never bigger than that of the Kelvin wave forced at the same instant. Furthermore, the Kelvin wave they will compete against at the east was forced later and so will be even stronger due to the positive feedback. So how can the Rossby signal win?

The answer lies in the incremental way it achieves this goal. After the onset of an anomaly the Rossby wave will always tend to diminish the Kelvin wave

signal. When the Kelvin wave hits the eastern boundary (and mass is exported poleward), the subsequently forced Kelvin wave is weaker than expected from the direct feedback alone. Its effect is diminished further by the Rossby wave signal which was reflected at the west and now reaches the forcing region as a negative Kelvin wave. The restoring effects of the Rossby waves accumulate. As long as the feedback is not too strong this can bring the thermocline back to zero and so lead to an oscillation. "Constant dripping wears away the stone," as the saying goes.

We have not yet taken account of the Rossby waves formed at the eastern boundary out of the Kelvin wave. We may consider these as acting on the forced Rossby waves in a way similar to the forced Rossby waves on the Kelvin signal. If the east coast were a perfect reflector and the wave speed were the same, then these waves would cancel out the restoring effect of the forced Rossby waves and pure growth could happen. But the east coast is an inefficient reflector. A lot of energy goes into higher very slow Rossby modes and is lost for a long time. The cancellation is only partial and growing oscillations can occur. In addition, the slower speed of the Rossby waves compared to the Kelvin wave delays the signal of the eastern reflection, and so further reduces the influence of this boundary. An oscillation becomes even more likely.

Now consider the decisive role of the Rossby wave for the onset of the event. Consider the moment when the forcing amplitude just passes through zero and turns eastward, generating a positive Kelvin wave. Since the directly forced Kelvin part cannot turn positive until after the height at the east does, the turnabout must be initiated by the indirect Rossby waves; the indirect component is essential to the initiation of an event. This positive Rossby signal had to have been generated at an earlier period when the winds were westward.

It is clear from the above that the Rossby contribution to the height at the east leads the Kelvin contribution. An elementary consideration of the sum of two waves of the same frequency will convince the reader that the phase of the total height and hence the wind is between the two. [A further consequence of the Rossby component leading the wind is that the zonal integral of the height along the equator, which depends heavily on the Rossby contribution, will lead the wind. This feature was emphasized by Zebiak and Cane (1987).] The maximum wind (i.e, the peak of the warm event) comes at the phase of the oscillation where the two components are maximally reinforcing. Though the direct Kelvin contribution rises to a peak thereafter (in the time interval $1\text{-}x_c$ it takes to cross from the forcing to the boundary), the decline in the Rossby component ensures that the wind will continue to subside. Eventually it again crosses zero and enters the negative phase of the cycle.

In this account the origins of a warm event may be traced back to the largely off-equatorial Rossby wave positive height anomalies generated during previous cold episodes. The directly forced Kelvin wave contributes to the strength and duration of the event, but if it is too dominant (as happens when the coupling is very strong or x_c is too far to the east) then pure growth replaces the oscillation. We have not emphasized it, but the Rossby waves generated at the eastern boundary during the last event can also contribute a positive height signal to the initiation of the present one. Note that Battisti and Hirst (1989) and Suarez and Schopf (1988) leave this effect out altogether; we agree that it is not essential. [A different view is that of Graham and White (1988).]

Many of the features of the system we have modeled are inherent in its geometry. The wind forcing responds to oceanic variables in a region to the east of it along the equator. In this setup Kelvin waves are the only means of carrying any signal east of the forcing to the sensitive region. Since the only instabilities involving solely the directly forced Kelvin waves are pure growing ones, the oscillations rely on the indirect path of Rossby waves forced in the ocean interior and propagating to the western boundary where they can be reflected as Kelvin waves. The same geometry is found in many other models for ENSO, including all of the numerical and reduced models listed earlier.

The obvious question is whether this geometry fits the observed ENSO. The elements we have emphasized are certainly present: the major wind anomalies are in the center of the equatorial Pacific and it is generally accepted that they can be explained as part of the atmospheric response to SST anomalies in the eastern equatorial Pacific. The interaction we have modeled, which is consistent within the class of models we listed earlier, is a plausible candidate explanation not inconsistent with what is known about ENSO. There are other features, however, which seem to appear with each ENSO event and are not part of this scheme. Perhaps they are inconsequential, but perhaps not. We would call attention to the warming on the equator in the vicinity of the date line which seems to be present at the early stages of ENSO events. The winds associated with this are to some extent collocated with it. With this geometry Rossby waves and Ekman fluxes can have a direct effect and so different interactions become possible. To our knowledge, no numerical models capture this feature and no reduced models have been used to investigate it (but cf. Hirst 1987, Model II; Rennick and Haney 1985).

These issues merit attention, but before turning our attention to them, we will first extend the present reduced model to allow a more strenous comparison with the ZC numerical model. This is done in a companion paper (Münnich et al. 1990), where it is shown that adding a nonlinear relation between wind stress and height to the framework set out here recreates much

of the interesting behavior of the numerical model, including the tendency to exhibit aperiodic oscillations.

Acknowledgments. We thank David Battisti and Tony Hirst for valuable discussions, and Virginia DiBlasi for preparing the manuscript. This work was supported by the NSF Grant No. ATM-8612570 and TOGA Grant No. NA-87-AA-D-AC0-81.

APPENDIX A

Nonrotating Model

Consider a nonrotating shallow water system bounded at $x = 0$ and $x = 1$ and forced by a stress of amplitude A at $x = x_c$. Further suppose a uniform basic state current U. Thus the scaled equation governing small perturbations:

$$u_t + Uu_x + h_x = A(t)\delta(x - x_c)$$
$$h_x + Uh_x + u_x = 0. \tag{A1}$$

The free solutions are eastward propagating solutions with $u = h$ and speed $1 + U$ and westward propagating wave with $u = -h$ and speed $1 - U$. We will refer to the former as K-waves and the latter as R-waves. Now rescale time by $(1 + U)$ so 1 time unit is the time it takes a K-wave to cross the basin. Also, let $\alpha = (1 + U)/(1 - U)$, the ration of the K-wave to the R-wave speed. Neglecting boundary conditions for the moment, the solution to (A1) is

$$u = h = A[t - (x - x_c)] \quad x > x_c$$
$$u = -h = A[t + \alpha(x - x_c)] \quad x < x_c. \tag{A2}$$

In the usual problem the boundary conditions are $u = 0$ at $x = 0, 1$. We generalize here by allowing the boundaries to be imperfect reflectors with reflection coefficients r_w at $x = 0$ and r_e at $x = 1$; e.g., a K-wave of amplitude (a_0) incident on the boundary at $x = 1$ is reflected as an R-wave of amplitude—$r_e a_0$. Denoting $h\,(x = 1)$ by h_e and using (A2) we obtain

$$h_e(t) = A[t - (1 - x_c)] - r_w A[t - (1 + \alpha x_c)] + r_e r_w h_e[t - (1 + \alpha)]. \tag{A3}$$

Substituting $A = \kappa h$ as in the body of the paper and letting $h_e(t) = e^{\sigma t}$ yields

$$1 = \kappa\{e^{-\sigma(1-x_c)} - r_w e^{-\sigma(1+\alpha x_c)}\} + r_w r_e e^{-\sigma(1+\alpha)}. \tag{A4}$$

As in section 3 we differentiate (A4) with respect to σ and set $\partial\kappa/\partial\sigma = 0$ to find the minimum $\kappa = \kappa_m$ that allows pure growth. If this value, $\sigma = \sigma_m$ is positive, then there are growing, oscillating modes for $\kappa < \kappa_m$. If $\sigma_m \leqslant 0$ then there is a strip around the positive real axis that contains no solutions of (A4). We conclude that the low frequency oscillating modes for $\kappa < \kappa_m$ are neutral or decaying.

Define

$$a = 1 + \frac{(\alpha - 1)}{2} x_c$$
$$b = \frac{(1 + \alpha)}{2} x_c$$
$$e^{\vartheta_w} = r_w^{-1/2} \tag{A5}$$

and rewrite (A4) as

$$\kappa = 2\frac{r_w^{-1/2}}{2} e^{a\sigma} \frac{1 - r_e r_w e^{-\sigma(1+\alpha)}}{\sinh(b\sigma + \vartheta_w)}. \tag{A6}$$

Setting $\partial\kappa/\partial\sigma = 0$ yields the relation

$$\tanh(b\sigma + \vartheta_w) = \frac{b}{a} \frac{1 - r_e r_w e^{-\sigma(1+\alpha)}}{1 + r_e r_w \left[\frac{1+\alpha}{a} - 1\right] e^{-\sigma(1+\alpha)}}. \tag{A7}$$

(LHS) (RHS)

We are interested in knowing whether there is a solution to (A7) with $\sigma > 0$. Note that as $\sigma \to \infty$, LHS $\to 1$ and RHS $\to b/a$ and since $x_c < 1$, $b/a < 1$. Hence, as $\sigma \to \infty$, LHS > RHS. Since both LHS and RHS do not decrease with increasing σ it follows that if LHS < RHS at $\sigma = 0$ there is a $\sigma > 0$ where LHS = RHS.

We first consider the case $r_e < 1$. Then at $\sigma = 0$

$$\text{LHS} = \tanh\vartheta_w = \frac{1 - r_w}{1 + r_w};$$
$$(\text{RHS}) = b\frac{1 - r_e r_w}{(\alpha + 1 - a) r_e r_w}.$$

Hence there is a growing oscillating mode if

$$\frac{1 - r_w}{1 + r_w} < b\frac{1 - r_e r_w}{a + (\alpha + 1 - a) r_e r_w}. \tag{A8}$$

The inequality (A8) holds for all $x_c \neq 0$ if $r_w = 1$, perfect reflection at the west (since we have assumed $r_e < 1$). Especially if, as in SS and BH, $r_e = 0$, then the conditions (A8) is met. Also, the larger α, (the ratio of the K-wave to R-wave speed) the more readily (A8) is satisfied. If the two wave speeds are equal, $\alpha = 1$ and (A8) becomes

$$\frac{1 - r_w}{1 + r_w} < x_c \frac{1 - r_e r_w}{1 + r_e r_w}; \tag{A9}$$

even with weak reflection at the west oscillations are possible if r_e is small enough and the forcing is far enough to the east.

If $r_e = r_w = 1$ the above analysis breaks down since LHS = RHS = 0 at $\sigma = 0$. In this case we expand RHS and LHS around $\sigma = 0$.

Now

$$\text{LHS} = b\sigma + O(\sigma^3)$$

$$\text{RHS} = b\frac{1 - e^{-(\alpha+1)\sigma}}{a + (\alpha + 1 - a)e^{-(\alpha+1)\sigma}}$$

$$= \frac{b}{\alpha + 1}\left[\left((\alpha + 1)\sigma - \frac{(\alpha + 1)^2}{2}\sigma^2\right) \times [1 + (\alpha + 1 - a)\sigma] + O(\sigma^3)\right],$$

$$= b\sigma + b(\alpha - 1)(1 - x_c)\frac{\sigma^2}{2} + O(\sigma^3). \quad \text{(A10)}$$

The latter is larger than the former for σ sufficiently small if $\alpha > 1$. So for slower speed of the R-wave there are growing oscillations even if $r_e = r_w = 1$.

APPENDIX B

Some Other Formulations of Thermodynamics or Atmospheric Response

We begin with the difference between the thermodynamics used here [Eq. (1′)] and that used by BH and SS [Eq. (1″)]. Making the same assumptions as in the text (most importantly, that T_e depends on h_e) allows (1″) to be written in the form

$$\left(\tau_1\frac{\partial}{\partial\tau} + 1\right)A(t) = \kappa h_e(t). \quad \text{(B1)}$$

Equation (B1) reduces to that used here [Eq. (3)] if $\tau_1 = 0$. BH obtained the equivalent of (B1) (together with estimates for κ and τ_1) from (1) and the results of Battisti's (1988) version of the Zebiak and Cane (1987) numerical model. Theirs is a more thorough derivation than ours or that of Schopf and Suarez (1989). Nonetheless, such a drastic simplification cannot be expected to reproduce all the nuances of the more complete model. Furthermore, while it perhaps can capture the essence of the periodic behavior of Battisti's (1988) version of the ZC model, such a linear model obviously cannot exhibit the aperiodicity of the original ZC model, let alone the richer behavior of the natural system.

The time derivative in (B1) allows A to lag h_e. An additional delay can be posited on the grounds that while h_e has an almost immediate effect on the temperature right at the equator, it takes additional time τ_2 for meridional currents, diffusion, etc. to spread the temperature change over the area with ultimately affects the atmosphere; then

$$\left(\tau_1\frac{\partial}{\partial t} + 1\right)A(t) = \kappa h_e(t - \tau_2). \quad \text{(B2)}$$

This effect is not considered by BH. In addition, they ignore the time $(1 - x_c)$ it takes a Kelvin wave to propagate from the wind forcing region to the eastern boundary. From their Fig. 8, this time is approximately 0.4 in nondimensional units of Kelvin wave crossing times. (We took $x_c = 0.5$ as typical of observed ENSO events; the model wind anomaly peaks too far east.) Since BH additionally simplify the ocean dynamics by including only one Rossby wave and ignoring reflections at the east their dynamics reduce to [their Eq. (2.4)]:

$$h_e(t) = a_L A(t) - a_w A(t - \tau). \quad \text{(B3)}$$

Combining this with the thermodynamics (B1) yields their Eq. (2.9):

$$\frac{\partial T}{\partial t} = -bT(t - \tau) + cT. \quad \text{(B4)}$$

Our analogous one Rossby mode model is (47) with $r_e = 0$ and $\tau = 1 + \alpha x_c$; taking $\Delta t = 1 - x_c$ and $\tau = x_c(\alpha - 1)$ allows it to be written as

$$h(t + \Delta\tau) = \kappa h(t) - r_w\kappa h(t - \tau). \quad \text{(B5)}$$

Taking

$$\frac{r_w\kappa}{\Delta t} = b; \quad \frac{\kappa - 1}{\Delta t} = c$$

and

$$\frac{\partial h}{\partial t} \approx \frac{h(t + \Delta t) - h(t)}{\Delta t} \quad \text{(B6)}$$

reveals the essential similarity of the two approaches. Equation (B5) is a good approximation to (B4) for the cases of greatest interest, which have long periods and growth rates (long compared with Δt; hence $|\sigma\Delta t| \ll 1$).

The conclusion is that the differing thermodynamics make no important qualitative differences, though, once again, the periods and growth rates are quantitively sensitive to such differences. If we had replaced (1′) by the more elaborate thermodynamic/atmospheric response model (B2), then instead of $\kappa^2 = G^{-2}$ as in (18) we would have had

$$\kappa^2 = G^{-2}(\sigma)[e^{\sigma\tau_2}(\sigma\tau_1 + 1)]^2. \quad \text{(B7)}$$

Finding the minimum κ allowing pure growth [cf. (18)ff] now yields

$$0 = \frac{\partial}{\partial\sigma}\left(\frac{1}{2}\kappa^2\right)$$

$$= \frac{\partial G^{-2}}{\partial\sigma}[e^{\sigma\tau_2}(\sigma\tau_1 + 1)]^2 + G^{-2}[e^{\sigma\tau_2}(\sigma\tau + 1)]^2 \times \left\{2(\tau_1 + \tau_2) - \frac{2\sigma{\tau_1}^2}{1 + \sigma\tau_1}\right\}. \quad \text{(B8)}$$

If $\sigma\tau_1 \ll 1$, then consistent with the discussion of (B4) and (B5), the time derivative (τ_1) and the delay (τ_2) have the same effect. If $2(\tau_1 + \tau_2) < O(\mu^{1/3})$ then

a straightforward perturbation analysis yields [cf. (21), (23)]:

$$\sigma_m = \mu^{1/3} - \frac{2}{3}(\tau_1 + \tau_2)$$

$$\kappa_m = (2 + 3\mu^{2/3})^{1/2}[1 + \mu^{1/3}(\tau_1 + \tau_2)].$$

With the added delays the transition growth rate is diminished and the coupling strength increased, but there are no important qualitative changes. The effect is similar to that obtained by moving x_c westward in the western half of the basin (cf. Fig. 6), which also increases the time between the forcing by the wind and the eastern ocean response.

REFERENCES

Battisti, D. S., 1988: Dynamics and thermodynamics of a warming event in a coupled tropical atmosphere-ocean model. *J. Atmos. Sci.*, **45**, 2889–2919.

Bjerknes, J., 1966: A possible response of the atmospheric Hadley circulation to equatorial anomalies of ocean temperature. *Tellus*, **18**, 820–829

——, 1969: Atmospheric teleconnections from the equatorial Pacific. *Mon. Wea. Rev.*, **97**, 163–172.

——, 1972: Large-scale atmospheric response to the 1965-65 Pacific equatorial warming. *J. Phys. Oceanogr.*, **15**, 1255–73.

Cane, M. A., and S. E. Zebiak, 1987: Deterministic prediction of El Niño events. *Atmospheric and Oceanic Variability*, H. Cattle, Ed., Roy. Meteor. Soc./Amer. Meteor. Soc., 153–182.

——, and D. W. Moore, 1981: A note on low frequency equatorial basin modes. *J. Phys. Oceanogr.*, **11**, 1578–1584.

——, and E. S. Sarachik, 1981: The response of a linear baroclinic equatorial ocean to periodic forcing. *J. Mar. Res.*, **39**, 651–693.

——, S. E. Zebiak and S. C. Dolan, 1986: Experimental forecasts of El Niño. *Nature*, **321**, 827–832.

Gill, A. E., and E. Rasmussen, 1983: An estimation of sea-level and sea-current anomalies during the 1972 El Niño and consequent thermal effects. *J. Phys. Oceanogr.*, **13**, 586–605.

Graham, N. E., and W. B. White, 1988: The El Niño/Southern Oscillation as a natural oscillation of the tropical Pacific ocean/atmosphere system: Evidence from observations and models. *Science*, **240**, 1293–1302.

Harrison, D. E., and P. S. Schopf, 1984: Kelvin-wave-induced anomalous advection and the onset of surface warming on El Niño event. *Mon. Wea. Rev.*, **112**, 923–933.

Hirst, A. C., 1986: Unstable and damped equatorial modes in simple coupled ocean–atmosphere models. *J. Atmos. Sci.*, **43**, 606–630

——, 1987: Slow instabilities in tropical ocean basin—global atmosphere models. *J. Atmos. Sci.*, **455**, 830–852.

Latif, M., J. Biercamp and H. von Storch, 1988: The response of a coupled ocean–atmosphere general circulation model to wind bursts. *J. Atmos. Sci.*, **45**, 964–979.

Münnich, M., M. A. Cane and S. E. Zebiak, 1989: A study of self-excited oscillations in a tropical ocean-atmosphere system. Part II: Nonlinear cases. *J. Atmos. Sci.*, in press.

Rennick, M. A., and R. L. Haney, 1985: Stable and unstable air–sea interaction in the equatorial region. *J. Atmos. Sci.*, **43**, 2937–2943.

Schopf, P. S., and M. J. Suarez, 1988: Vacillations in a coupled ocean–atmosphere model. *J. Atmos. Sci.*, **45**, 549–566.

——, and ——, 1990: Ocean wave dynamics and the timescale of ENSO. *J. Phys. Oceanogr.*, in press.

Suarez, M. J., and P. S. Schopf, 1988: A delayed action oscillator for ENSO. *J. Atmos. Sci.*, **45**, 3283–7.

Wakata, Y., 1989: On the instability problem in simple air–sea coupled models with an oceanic surface boundary layer. *J. Meteor. Res. Japan*, in press.

Wyrtki, K., 1975: El Niño—The dynamic response of the equatorial Pacific Ocean to atmospheric forcing. *J. Phys. Oceanogr.*, **5**, 572–84.

Zebiak, S. E., 1984: Tropical atmosphere-ocean interaction and the El Niño/Southern Oscillation phenomenon. Ph.D. thesis, Massachusetts Institute of Technology, 261 pp.

——, and M. A. Cane, 1987: A model El Niño–Southern Oscillation. *Mon. Wea. Rev.*, **115**, 2262–2278.